CARBON letters

Note

Carbon Letters Vol. 23, 74-78 (2017)

Effects of synthesis pressure conditions on the preparation of graphene-like carbonaceous materials from organic liquid precursors by a solvothermal method

Kwan-Woo Kim[1,2], Byoung Suhk Kim[2], Sang Won Lee[1], Dong Chul Chung[1] and Byung-Joo Kim[1,3,♠]

[1]Multifunctional Carbon Materials Division, Korea Institute of Carbon Convergence Technology, Jeonju 54853, Korea
[2]Department of Organic Materials & Fiber Engineering, Chonbuk National University, Jeonju 54896, Korea
[3]Department of Carbon and Nano Materials Engineering, Jeonju University, Jeonju 55069, Korea

Key words: graphene, solvothermal, synthesis, organic liquid precursor, supercritical

Article Info
Received 5 November 2016
Accepted 23 March 2017

♠Corresponding Author
E-mail: kimbj2015@gmail.com
Tel: +82-63-219-3710

Open Access
DOI: http://dx.doi.org/10.5714/CL.2017.23.074

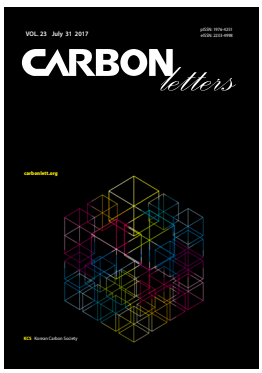

http://carbonlett.org

pISSN: 1976-4251
eISSN: 2233-4998

Carbon materials with at least one dimension of 1–100 nm are called carbon nanomaterials. A significant body of previous research in physics, chemistry and biology has demonstrated that the properties of nano-composites are significantly different than those of the bulk materials [1]. Some unique phenomena, such as the quantum tunneling effect, and surface effects, have also been observed, and attributed to the large surface area and small size of the carbon nanomaterials. It has been reported that such nanomaterials exhibit high temperature sensitivity, high ductility, large surface area, high strain resistance, and low electrical resistivity [2]. Because of these unique features, the potential range of carbon nanomaterial applications is very extensive.

Carbon nanotubes (CNTs), carbon nanofibers and graphene are the more commonly used carbon nanomaterials [3,4]. Among them, graphene has attracted considerable interest over the last few years due to its extraordinary electrical, thermal, and mechanical properties, which arise from its unique structure [5,6].

Graphene is a single layer of sp^2-bonded carbon atoms packed into a benzene-ring structure, and has recently become one of the most appealing stars in material science [7,8]. Graphene has attracted attention because of its interesting properties and potential applications. Due to its huge surface area (calculated value, 2630 m^2/g), excellent electric conductivity [5,9], and mechanical strength, graphene has shown great application potential in many fields, including electronic devices [10,11], energy storage and conversion [12,13], and bio application [14].

Since the first report on the synthesis of graphene sheets by the mechanical cleavage method in 2004 [15], a wide range of additional techniques have been reported. For example, single/ multi-layer graphene sheets have been grown epitaxially by the chemical vapor deposition of hydrocarbons on metal and nonmetal substrates [16], by substrate-free deposition [17], and the thermal decomposition of SiC [18,19]. In some early studies [20,21], these production methods resulted in low yields of carbon nanosheets, and contamination with other carbon allotropes such as CNTs. Recently, petal-like carbon nanosheets have been produced in macroscopic quantities by an arc-discharge reaction [22], and expanded graphite nanosheets have been produced from various graphite intercalation compounds submitted to brute thermal shock [23-25]. In addition, well-separated graphene sheets on substrates, i.e., carbon nanowalls, were recently synthesized using a microwave plasma enhanced chemical vapor deposition method, and by a hot filament chemical vapor deposition method [26-28]. These synthetic methods, however, required high temperature, complicated instruments, or metal catalysts. Most of these techniques make use of highly oriented pyrolytic graphite as a starting material, and involve labor-intensive preparations. Given the lack of a reliable top-down approach for the large-scale production of graphene, attention has turned to bottom-up approaches that might be able to deliver the economies of scale that are found in the chemical and pharmaceutical industries [29].

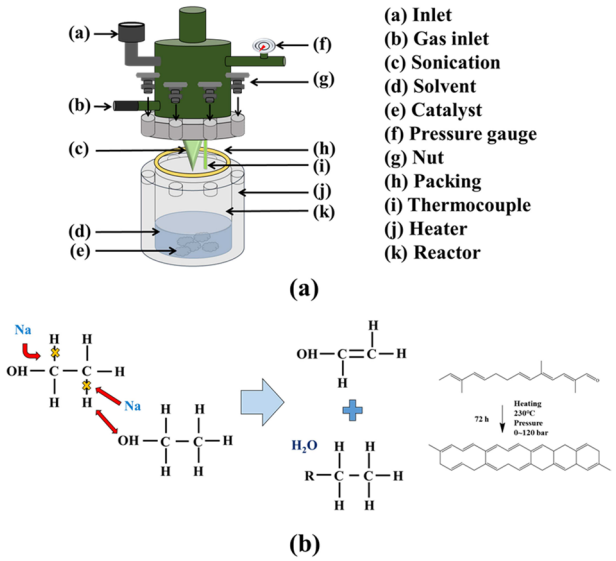

Fig. 1. (a) Schematic diagram of the self-produced reactor. (b) The reaction mechanism of aromatic groups and graphene structure in the presence of the sodium catalyst and ethanol precursors.

Choucair et al. [29] have reported a graphene production method at high pressure using sodium catalysts and ethanol precursors for mass production. However, the report on the graphene synthesis behavior didn't exhaustively cover the effects of synthetic pressure on the graphene formation.

Here, we report the direct chemical synthesis of graphene-like carbonaceous material nanosheets with various reaction pressure conditions in a bottom-up approach, based on a common organic liquid precursors and metal catalyst. The precursors and catalyst are reacted to give an intermediate solid that is then pyrolyzed, yielding a fused array of the sheets with graphene-like structures that are dispersed by mild sonication. The ability to produce bulk graphene-like samples from nongraphitic precursors with a scalable, low-cost approach should take us a step closer to practical applications of graphene.

All of the solvothermal reactions in this study were performed in a self-produced reactor which has a maximum volume of 200 mL. A schematic diagram of the self-produced reactor is illustrated in Fig. 1a. A typical synthesis consists of heating a 1:1 molar ratio of sodium (7647-1405; Daejung Chem., Korea) 2 g and ethanol (99.5%; Sigma-Aldrich, USA) 5 mL in a sealed reactor vessel at a temperature above 230°C for 72 h. This yields a solid solvothermal product (the graphene precursor). Samples of the solvothermal product were fabricated at different pressures, of 1, 20, 40, and 60 bar. This material was then rapidly pyrolyzed, and the remaining product washed with deionized water at least three times. The supended solid was then vacuum filtered and dried in a vacuum oven at 120°C for 24 h. The final yield of graphene was approximately 0.1 g per 1 mL of ethanol, typically yielding ~0.5 g per solvothermal reaction. The reaction mechanism of the sodium with ethanol, which introduces ethanol reaction groups and carbon-to-carbon double bonds, is illustrated in Fig. 1b.

The functional groups on the graphene-like materials synthesized under different pressure conditions were confirmed and analyzed using a Fourier transform infrared spectrometer (FT-IR; Nicolettm id tm10, Thermo Scientific, USA) at 4000–500 cm^{-1} wavelengths.

The differences in the structure of the graphene-like materials synthesized under different pressure conditions were determined using a wide-angle X-ray diffractometer (XRD; Empyrean, PANalytical, the Netherlands), employing a Empyrean X-ray diffractor with a customized auto-mount and a Cu Kα radiation source at 30 kV and 20 mA. Diffraction patterns were collected within diffraction angles from 20 to 80° with a speed of 2°/min.

Raman spectroscopy is a very effective method for investigating and determining the precise nanostructures of carbonaceous materials. The measurement area was chosen near to the mark point using a camera in a Raman microscope (NTegra; NT-MDT, Russia). Nano-Raman spectroscopy measurements were taken at room temperature in Raman scattering geometry with a changing polarizability. All of the samples were prepared and measured in powder form. Raman was performed using a green (532 nm) laser excitation wavelength, and a magnification of ×100. Scans were taken in the range of 500–4000 cm^{-1}.

Transmission electron microscopy (TEM) images were obtained using high resolution Bio-TEM (H-7650; Hitachi, Japan) at an acceleration voltage of 200 kV. The samples used for TEM characterization were prepared by placing a drop of prepared solution on a carbon-coated copper grid and drying at room temperature.

The obtained FT-IR spectra of the graphene synthesized under different pressure conditions indicated an increase in C–C stretch groups (in-ring) from 1400 to 1600 cm^{-1} and alkyl C-H groups (1650–1740 cm^{-1}), due to the formation of C=C–C stretch groups (in the aromatic ring), as shown in Fig. 2. The IR spectra show that there was an increase in aromatic ring reaction after the pressure was increased, as evidenced by C=C–C bonding, arising from tightly bound sites in the graphene-like materials.

Fig. 3 shows the Raman spectra results of the graphene-like materials synthesized under different pressure conditions, with marks indicating *D* (defect), *G* (graphite), and 2*D* peaks. Ra-

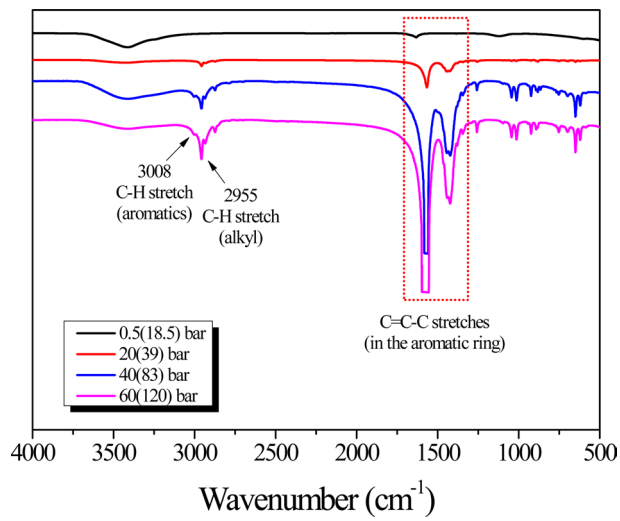

Fig. 2. Fourier transform infrared spectroscopy results of the graphene synthesized under different pressure conditions.

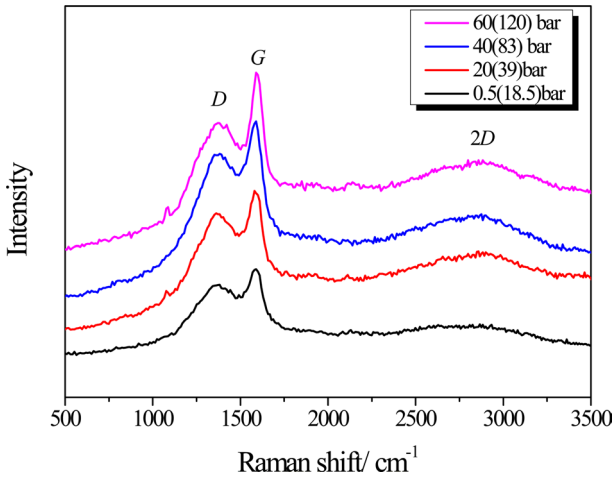

Fig. 3. Raman spectra results of the graphene synthesized under different pressure conditions.

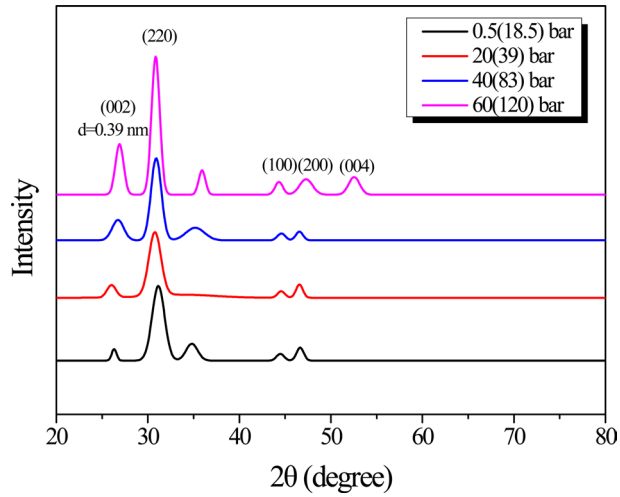

Fig. 4. X-Ray diffraction patterns of the graphene synthesized under different pressure conditions.

man spectra is limited in that the size of the laser focal point is typically micron scale. In addition, materials that are truly nanoscale inevitably have very high transmissions of visible light. The combination of these factors can result in materials of very different nanostructure having inherently similar Raman spectra [30,31].

The most noticeable part of Raman data of carbonaceous materials is the *G* peak near 1580 cm^{-1} and the *D* peak near 1340^{-1}. In addition, the 2*D* peak due to the second scattering, in which two *D* mode phonons are emitted, is often used for graphene Raman data. 2*D* peaks are used to identify single-layer graphene. The observation of stronger peaks with narrower widths increases the likelihood that the scanned sample is single-layer graphene.

For graphitic materials, the intensity of the *G* band, caused by the in-plane stretching motion between pairs of sp^2 carbon atoms, is very much greater than that of the *D* band, which is believed to be due to a double-resonance and enhanced by edge effects and the dangling bonds of the sp^2 carbon sites. The rationale then follows that if $I_G >> I_D$, then the number of defect sites must be very much lower than graphitic sites. However, the number of edge sites rapidly increases as the lateral dimensions of the sheets decrease, hence populating the *D* band.

In this respect, carbonaceous materials of different form, but similar aspect ratio, may display a similar value of I_G/I_D. The situation is further complicated by the fact that Raman peaks due to the carbon-carbon stretches in amorphous sp^3 hybridized carbon, also lie within this spectral window. Finally, graphene sheets have an inherent tendency to overlay each other due to favorable π–π interactions, resulting in a high probability that numerous edge sites will be illuminated within any given focal point of micrometer dimensions, yielding $I_G \sim I_D$. The observation of spectra having broad peaks of similar form across carbonaceous materials requires discriminatory characterization techniques, such as microscopy and electron diffraction, to confirm the presence of individual graphene sheets.

In the present study, structural analyses of the graphene-like material sheets obtained via synthesis under different pressure conditions were performed using XRD analysis. In Fig. 4, only the carbon crystal peaks inherent to graphite were observed; the XRD pattern of graphene-like material has a strong peak at 2θ=25–27°. The figure shows the intensity of graphene synthesized at high pressure (002) is greater, with a sharp and strong diffraction peak, compared with that of graphene-like materials synthesized at low pressure. When the observed XRD data of the synthesized graphene-like material sheets were viewed, it was confirmed that there were no other crystal plane diffraction peaks. This result indicates that there were no crystals containing oxygen or other functional groups in the graphene-like material sheets.

The morphological characteristics of graphene-like material powders as a function of initial reaction pressures were analyzed using optical images (Fig. 5a) and TEM (Fig. 5b) images of the sample synthesized at 60 bar. The TEM image of the synthesized graphene-like materials shows a sheet-like morphology; its transparency depends on the number of laminated graphene sheets in the irradiated region, which is about 100 nm (Fig. 5b). Dark areas represent thick stacked nanostructures in the gra-

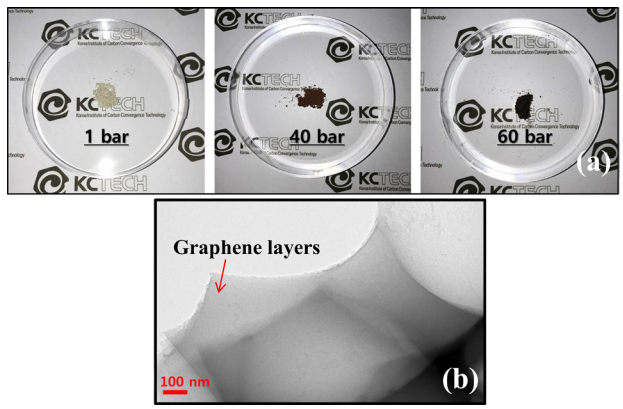

Fig. 5. (a) Optical images of the samples as a function of initial reaction pressures, (b) transmission electron microscopy images of the sample synthesized at 60 bar.

phene layer, while areas of high transparency represent a much thinner layer of film in the graphene sheet.

Using these results, the effect of the reaction pressure on the formation of graphene-like materials was investigated, following the bulk graphene synthesis using organic liquid precursors and metal catalysts. It was found that samples produced at an initial pressure of 40 bar and a reaction pressure of 80 bar or more had graphene-specific XRD and Raman patterns, and the highest levels of graphene were synthesized under a more severe condition, at an initial pressure of 60 bar and a reaction pressure of 120 bar. The reaction temperature for all samples was 230°C.

From the above experimental results, it was found that graphene mass synthesis using various organic precursors is possible, and an optimum reaction pressure is present.

Conflict of Interest

No potential conflict of interest relevant to this article was reported.

Acknowledgements

This study was supported by the "National Research Foundation of Korea (Project No. 2015M3A7B4049716)" funded by the Korea government (MSIP), Republic of Korea.

References

[1] Yang J, Tighe S. A review of advances of nanotechnology in asphalt mixtures. Procedia Soc Behav Sci, **96**, 1269 (2013). https://doi.org/10.1016/j.sbspro.2013.08.144.

[2] Yang Z, Hollar J, Shi X. Surface-sulfonated polystyrene microspheres improve crack resistance of carbon microfiber-reinforced Portland cement mortar. J Mater Sci, **45**, 3497 (2010). https://doi.org/10.1007/s10853-010-4386-7.

[3] Li R, Xiao X, Amirkhanian S, You Z, Huang J. Developments of nano materials and technologies on asphalt materials: a review. Constr Build Mater, **143**, 633 (2017). https://doi.org/10.1016/j.conbuildmat.2017.03.158.

[4] Kim BJ, Lee YS, Park SJ. A gas control by metal nanoclusters-supported porous carbon nanofibers. Solid State Phenom, **119**, 5 (2007). https://doi.org/10.4028/www.scientific.net/ssp.119.5.

[5] Geim AK, Novoselov KS. The rise of graphene. Nat Mater, **6**, 183 (2007). https://doi.org/10.1038/nmat1849.

[6] Kim BJ, Byun JH, Park SJ. Effects of graphenes/CNTs co-reinforcement on electrical and mechanical properties of HDPE matrix nanocomposites. Bull Korean Chem Soc, **31**, 2261 (2010). https://doi.org/10.5012/bkcs.2010.31.8.2261.

[7] Zhu Y, Murali S, Cai W, Li X, Suk JW, Potts JR, Ruoff RS. Graphene and graphene oxide: synthesis, properties, and applications. Adv Mater, **22**, 3906 (2010). https://doi.org/10.1002/adma.201001068.

[8] Rao CNR, Sood AK, Subrahmanyam KS, Govindaraj A. Graphene: the new two-dimensional nanomaterial. Angew Chem Int Ed, **48**, 7752 (2009). https://doi.org/10.1002/anie.200901678.

[9] Cho YL, Lee JW, Park C, Song YI, Suh SJ. Study of complex electrodeposited thin film with multi-layer graphene-coated metal nanoparticles. Carbon Lett, **21**, 68 (2017). https://doi.org/10.5714/cl.2017.21.068.

[10] Meng X, Geng D, Liu J, Banis MN, Zhang Y, Li R, Sun X. Non-aqueous approach to synthesize amorphous/crystalline metal oxide-graphene nanosheet hybrid composites. J Phys Chem C, **114**, 18330 (2010). https://doi.org/10.1021/jp105852h.

[11] Chen D, Tang L, Li J. Graphene-based materials in electrochemistry. Chem Soc Rev, **39**, 3157 (2010). https://doi.org/10.1039/b923596e.

[12] Paek SM, Yoo EJ, Honma I. Enhanced cyclic performance and lithium storage capacity of SnO_2/graphene nanoporous electrodes with three-dimensionally delaminated flexible structure. Nano Lett, **9**, 72 (2009). https://doi.org/10.1021/nl802484w.

[13] Chen YL, Hu ZA, Chang YQ, Wang HW, Zhang ZY, Yang YY, Wu HY. Zinc oxide/reduced graphene oxide composites and electrochemical capacitance enhanced by homogeneous incorporation of reduced graphene oxide sheets in zinc oxide matrix. J Phys Chem C, **115**, 2563 (2011). https://doi.org/10.1021/jp109597n.

[14] Ren J, Zhang X, Chen Y. Graphene accelerates osteoblast attachment and biomineralization. Carbon Lett, **22**, 42 (2017). https://doi.org/10.5714/CL.2017.22.042.

[15] Novoselov KS, Geim AK, Morozov SV, Jiang D, Zhang Y, Dubonos SV, Grigorieva IV, Firsov AA. Electric field effect in atomically thin carbon films. Science, **306**, 666 (2004). https://doi.org/10.1126/science.1102896.

[16] Land TA, Michely T, Behm RJ, Hemminger JC, Comsa G. STM investigation of single layer graphite structures produced on Pt(111) by hydrocarbon decomposition. Surf Sci, **264**, 261 (1992). https://doi.org/10.1016/0039-6028(92)90183-7.

[17] Dato A, Radmilovic V, Lee Z, Phillips J, Frenklach M. Substrate-free gas-phase synthesis of graphene sheets. Nano Lett, **8**, 2012 (2008). https://doi.org/10.1021/nl8011566.

[18] Forbeaux I, Themlin JM, Debever JM. Heteroepitaxial graphite on 6H-SiC(0001): interface formation through conduction-band electronic structure. Phys Rev B, **58**, 16396 (1998). https://doi.org/10.1103/physrevb.58.16396.

[19] Van Bommel AJ, Crombeen JE, Van Tooren A. LEED and Auger electron observations of the SiC(0001) surface. Surf Sci, **48**, 463 (1975). https://doi.org/10.1016/0039-6028(75)90419-7.

[20] Ebbesen TW, Ajayan PM. Large-scale synthesis of carbon nanotubes. Nature, **358**, 220 (1992).

[21] Ando Y, Iijima S. Preparation of carbon nanotubes by arc-discharge evaporation. Jpn J Appl Phys, **32**, 107 (1993). https://doi.org/10.1143/jjap.32.l107.

[22] Ando Y, Zhao X, Ohkohchi M. Production of petal-like graphite sheets by hydrogen arc discharge. Carbon, **35**, 153 (1997). https://doi.org/10.1016/s0008-6223(96)00139-x.

[23] Nakajima T, Matsuo Y. Formation process and structure of graphite oxide. Carbon, **32**, 469 (1994). https://doi.org/10.1016/0008-6223(94)90168-6.

[24] Celzard A, Krzesiñska M, Bégin D, Marêché JF, Puricelli S. Furdin G. Preparation, electrical and elastic properties of new anisotropic expanded graphite-based composites. Carbon, **40**, 557 (2002). https://doi.org/10.1016/s0008-6223(01)00140-3.

[25] Liu GQ, Yan M. The preparation of expanded graphite using fine flaky graphite. New Carbon Mater, **17**, 13 (2002).

[26] Wu Y, Qiao P, Chong T, Shen Z. Carbon nanowalls grown by microwave plasma enhanced chemical vapor deposi-

tion. Adv Mater, **14**, 64 (2002). https://doi.org/10.1002/1521-4095(20020104)14:1<64::AID-ADMA64>3.0.CO;2-G.
[27] Kurt R, Bonard JM, Karimi A. Morphology and field emission properties of nano-structured nitrogenated carbon films produced by plasma enhanced hot filament CVD. Carbon, **39**, 1723 (2001). https://doi.org/10.1016/s0008-6223(00)00309-2.
[28] Shang NG, Au FCK, Meng XM, Lee CS, Bello I, Lee ST. Uniform carbon nanoflake films and their field emissions. Chem Phys Lett, **358**, 187 (2002). https://doi.org/10.1016/s0009-2614(02)00430-x.
[29] Choucair M, Thordarson P, Stride JS. Gram-scale production of graphene based on solvothermal synthesis and sonication. Nat Nanotechnol, **4**, 30 (2009). https://doi.org/10.1038/nnano.2008.365.
[30] Roy D, Chhowalla, Wang H, Sano N, Alexandrou I, Clyne TW, Amaratunga GAJ. Characterisation of carbon nano-onions using Raman spectroscopy. Chem Phys Lett, **373**, 52 (2003). https://doi.org/10.1016/s0009-2614(03)00523-2.
[31] Kawakami M, Karato T, Takenaka T, Yokoyama S. Structure analysis of coke, wood charcoal and bamboo charcoal by Raman spectroscopy and their reaction rate with CO_2. ISIJ Int, **45**, 1027 (2005). https://doi.org/10.2355/isijinternational.45.1027.